Electronic Supplementary Information

Alginate Nanoparticle Synthesis Using *n*-Heptane and Isopropyl Myristate/AOT Reverse Micelles: Impact of the Non-polar Solvent, Water Content, and pH on Particle Size and Cross-linking Efficiency

Fanny Melina Duque[a,b], N. Mariano Correa[a,b] and R. Dario Falcone[a,b]*

[a] Departamento de Química, Universidad Nacional de Rio Cuarto, Agencia Postal 3, C.P. X5804BYA, Ruta Nacional 36, km 601, Rio Cuarto, Córdoba, Argentina.

[b] Instituto de Desarrollo Agroindustrial y de la Salud (IDAS), Universidad Nacional de Río Cuarto, Agencia Postal 3, C.P. X5804BYA, Ruta Nacional 36, km 601, Río Cuarto, Córdoba, Argentina.

* Corresponding-Author: Dr. R. D. Falcone. E-mail: rfalcone@exa.unrc.edu.ar

Experimental Section

Preparation of AOT RMs solutions:

Stock solutions of AOT (0.1 M) in *n*-heptane or IPM were prepared by mass and volumetric dilution. Specific quantities of these stock solutions were then used to create individual RM solutions with varying amounts of water, denoted as $W_0 = [water]/[AOT]$. The addition of water and reactants to each micellar solution was carefully done using calibrated microsyringes. The resulting solutions exhibited a clear and homogeneous phase and were subsequently utilized in the synthesis experiments.

Preparation of ALG-NPs:

To test the optimal concentrations of reactants (sodium alginate and $CaCl_2$) inside the AOT RMs different experiments were performed varying the sodium alginate and $CaCl_2$ concentrations in n-heptane/AOT solutions, keeping constant the $[AOT] = 0.1$ M and the water content. Thus, sodium alginate was varied from $9x10^{-10}$ M to $2x10^{-7}$ M and $CaCl_2$ from $9x10^{-5}$ M to $2x10^{-3}$ M. In all cases, the concentrations evaluated provided stable AOT RMs and ALG-NPs with diameters in the range of 120-250 nm. Larger concentrations were not possible to prepare due to the polymer or the Ca^{2+} destabilizing the micellar system.

The identical aqueous solutions that were previously tested in AOT RMs were also examined in homogeneous media. Table S1 summarizes the experiments conducted at different concentrations of alginate and $CaCl_2$. Images of the final solutions after mixing the sodium alginate and $CaCl_2$ solutions are shown in Figure S1. It can be observed that a precipitate is detected in several solutions, which is attributed to gel/sediment formation. To avoid this phenomenon and preserve the stability of the AOT

RMs, the concentrations chosen in all subsequent experiments were [sodium alginate] = 9×10^{-8} M and [CaCl$_2$] = 9×10^{-4} M.

ALG-NPs inside AOT RMs were synthesized using the reverse micellar method adapted from a procedure previously with some modifications.[1,2] Initially, a micellar solution consisting of AOT and either n-heptane or IPM is prepared. An aqueous solution containing sodium alginate is then added to this micellar solution, and the resulting mixture is shaken for 5 minutes. Following this, an aqueous solution of CaCl$_2$ is introduced into the AOT, n-heptane, or IPM, and sodium alginate solution. The desired water content is achieved by incorporating pure water into the mixture. The resulting solution is then subjected to shaking at 25 °C for 2 hours. Subsequently, the nanoreactor containing the encapsulated nanoparticles is left undisturbed overnight. The following day, acetone is added to the solution to collapse the micellar system, which serves to remove the surfactant and organic solvent through decantation. To separate the ALG-NPs from the acetone solution, ultracentrifugation is performed at room temperature at a speed of 12,000 rpm. The resulting ALG-NPs are then washed with fresh acetone four times to ensure the removal of any remaining impurities. Finally, the ALG-NPs are dried at room temperature for 12 hours. No additional purification steps are taken, and the ALG-NPs are used as is.

Before use in the different studies, fresh ALG-NPs aqueous solutions were prepared in pure water, except when the pH was varied. In these experiments, the ALG-NPs obtained were resuspended in aqueous solutions at different pH values (4.2, 7.2, and 8.4) by adjusting with hydrochloric acid and sodium hydroxide accordingly.

DLS

The DLS measurements were carried out using an equipment model Malvern 4700 with a goniometer operating with OBIS 488 nm solid-state laser source (Coherent Inc.). The samples were filtered before the experiments using an Acrodisc with 0.45 μm nylon membrane (Sigma). To obtain statistically reliable results, 30 independent size measurements were taken for each of the samples. The scattering angle used was ninety degrees. The analysis of the particle size distribution in the medium involves utilizing the autocorrelation function and measuring the diffusion coefficient of the particles. The autocorrelation function can be obtained by analyzing the fluctuations in the intensity of scattered light over time. The decay rate of the correlation, known as G (equation S1), is directly influenced by the diffusion of the particles under investigation:

$$G = \int_0^\infty I(t)I(t+\tau)dt = B + Ae^{-2q^{2D\tau}}$$

(S1)

where B is the baseline, A is the amplitude, and D is the translational diffusion coefficient. The scattering vector (q) is determined by the following equation:

$$q = \frac{4\pi n}{\lambda_0}\sin\frac{\theta}{2}$$

(S2)

where n is the solvent refractive index, λ_0 is the vacuum wavelength of the laser, and θ is the scattering angle, usually 90 degrees. The speed of this Brownian motion is calculated and gives the translational diffusion coefficient D. This diffusion coefficient can be converted into an apparent hydrodynamic diameter (d_{app}) using the Stokes-Einstein equation (S3):[3–6]

$$d_{app} = \frac{kT}{3\pi\eta D}$$

(S3)

where k is the Boltzmann constant, T is the absolute temperature, and η is the solvent viscosity. The data obtained were evaluated using the CONTIN algorithm which is incorporated in the measurement instrument.

The polydispersity found for the different solutions investigated was always less than 5%.

The Zeta potential of the ALG-NPs was measured using a dynamic light scattering (ZetasizerNano ZS Malvern Instrument Ltd) operating at 633 nm.

FT-IR

FT-IR spectra were recorded with a Nicolet IMPACT400 FT-IR spectrometer. Sodium alginate and ALG-NPs samples were recorded in the range 400 - 4000 cm^{-1} using KBr pellets at room temperature. Each sample was obtained by co-adding 200 spectra at a resolution of 0.5 cm^{-1}.

TEM

To evaluate the morphology of the ALG-NPs obtained, TEM transmission electrical microscopy images were taken using a JEM-1400 Flash Transmission Electron Microscopy (JEOL, Tokyo, Japan) at a working voltage of 120 kV.

Table S1. Comparison of the sizes (d_{app}) and polydispersity index (PDI) values of the cross-linking reaction performed in bulk water. T = 25 ºC.

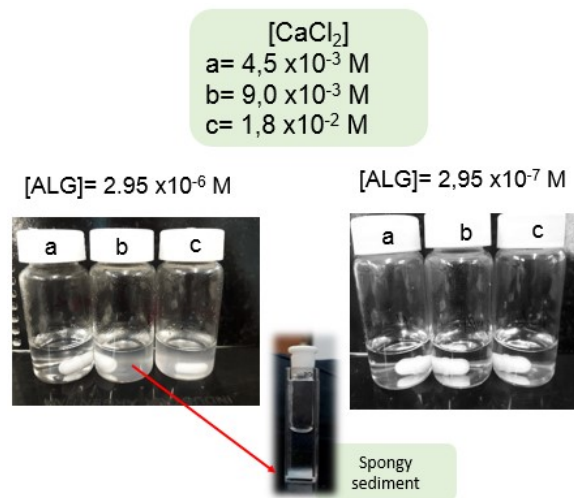| [ALG] / M	[CaCl$_2$] / M	d_{app} (nm)	PDI
9 x 10^{-8}	9 x 10^{-4}	30 ± 5 (9 %)	
		507 ± 4 (11 %)	1.00 ± 0.05
		1445 ± 10 (54 %)	
		415270 ± 150 (26 %)	
2 x 10^{-7}	9 x 10^{-3}	10 ± 4 (12.3 %)	
		2224 ± 10 (28.7 %)	1.00 ± 0.05
		37303 ± 100 (59 %)	

Figure S1. The visual appearance of the aqueous solutions after the crosslinking reaction of ALG with $CaCl_2$ in the absence of RMs.
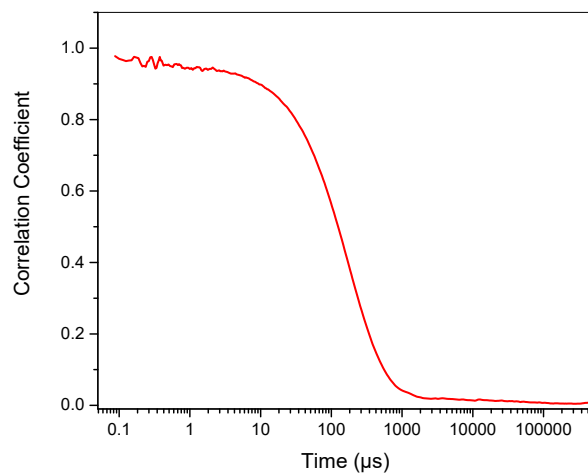
Figure S2. Autocorrelation function for a monodisperse sample of ALG-NPs synthesized in n-heptane/AOT/water RMs at $W_0 = 15$. $[CaCl_2] = 9x10^{-4}$ M, $[ALG] = 9x10^{-8}$ M.

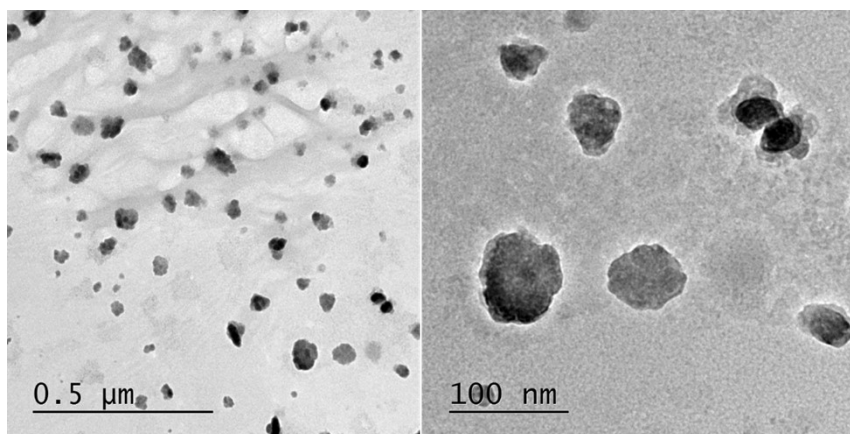**Figure S3.** TEM images of ALG-NPs synthesized in *n*-heptane/AOT/water RMs at $W_0 =$ 15. $[CaCl_2] = 9x10^{-4}$ M, $[ALG] = 9x10^{-8}$ M.

Table S2. Zeta potential values for ALG-NPs generated in AOT RMs. [AOT] = 0.1 M. [CaCl$_2$] = 9x10^{-4} M [ALG] = 9x10^{-8} M. T = 25 ºC.

Nanotemplate	W$_0$	Zeta Potential (mV)[a]
n-heptane/AOT/water	5	-56 ± 4
	15	-42 ± 2
IPM/AOT/water	5	-48 ± 3
	15	-40 ± 2

[a] Data corresponding to the NPs dissolved in water after removal of RMs.

REFERENCES

1   M. S. Orellano, C. Porporatto, J. J. Silber, R. D. Falcone and N. M. Correa, *Carbohydr Polym*, 2017, **171**, 85–93.

2   M. S. Orellano, G. S. Longo, C. Porporatto, N. M. Correa and R. D. Falcone, *Colloids Surf A Physicochem Eng Asp*, 2020, **599**, 124876.

3   A. V. Malm and J. C. W. Corbett, *Sci Rep*, , DOI:10.1038/s41598-019-50077-4.

4   J. Stetefeld, S. A. McKenna and T. R. Patel, *Biophys Rev*, 2016, 8, 409–427.

5   F. M. Agazzi, R. D. Falcone, J. J. Silber and N. M. Correa, *J Phys Chem B*, 2011, **115**, 12076–12084.

6   P. A. Hassan, S. Rana and G. Verma, *Langmuir*, 2015, **31**, 3–12.